ACS Catalysis

Letter

Cite This: ACS Catal. 2019, 9, 2962−2968

pubs.acs.org/acscatalysis

A Parsimonious Mechanism of Sugar Dehydration by Human GDP-Mannose-4,6-dehydratase

Martin Pfeiffer,[†] Catrine Johansson,[‡,§] Tobias Krojer,[‡] Kathryn L Kavanagh,[‡] Udo Oppermann,[‡,§,∥] and Bernd Nidetzky*[,†,¶]

[†]Institute of Biotechnology and Biochemical Engineering, Graz University of Technology, NAWI Graz, 8010 Graz, Austria

[‡]Structural Genomics Consortium, University of Oxford, Oxford OX3 7DQ, United Kingdom

[§]Botnar Research Centre, University of Oxford, Oxford OX3 7LD, United Kingdom

[∥]Freiburg Institute for Advanced Studies (FRIAS), University of Freiburg, 79085 Freiburg, Germany

[¶]Austrian Centre of Industrial Biotechnology, 8010 Graz, Austria

Supporting Information

ABSTRACT: Biosynthesis of 6-deoxy sugars, including L-fucose, involves a mechanistically complex, enzymatic 4,6-dehydration of hexose nucleotide precursors as the first committed step. Here, we determined pre- and postcatalytic complex structures of the human GDP-mannose 4,6-dehydratase at atomic resolution. These structures together with results of molecular dynamics simulation and biochemical characterization of wildtype and mutant enzymes reveal elusive mechanistic details of water elimination from GDP-mannose C5″ and C6″, coupled to NADP-mediated hydride transfer from C4″ to C6″. We show that concerted acid−base catalysis from only two active-site groups, Tyr_{179} and Glu_{157}, promotes a *syn* 1,4-elimination from an enol (not an enolate) intermediate. We also show that the overall multistep catalytic reaction involves the fewest position changes of enzyme and substrate groups and that it proceeds under conserved exploitation of the basic (minimal) catalytic machinery of short-chain dehydrogenase/reductases.

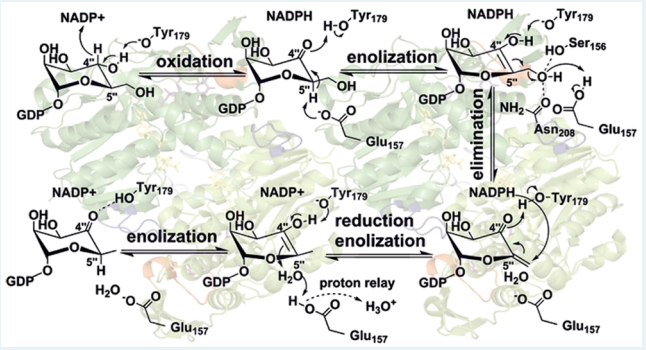

KEYWORDS: *β-elimination, carbohydrates, enzyme catalysis, reaction mechanism, sugar dehydratase, short-chain dehydrogenase/reductase*

6-Deoxysugars, prominently represented by the ubiquitous L-fucose,[1] are functionally important constituents of complex glycans and glycosylated natural products. Their biosynthetic pathways have in common that 4,6-dehydration of a hexose nucleotide precursor constitutes the first committed step.[2,3] The L-fucose (as GDP-L-fucose) is derived from GDP-D-mannose through an evolutionary conserved route via GDP-6-deoxy-α-D-*lyxo*-hexopyranos-4-ulose (GDP-4″-keto-6″-deoxy-mannose).[4−6] GDP-mannose 4,6-dehydratase (GMD) catalyzes the conversion of GDP-mannose.[5] The basic mechanism of GMD appears to be universally used by sugar 4,6-dehydratases.[2,3] It involves three catalytic steps (Figure 1a). The GDP-mannose is initially oxidized at C4″ by a $NADP^+$ cofactor tightly bound to the enzyme. Water is eliminated from GDP-α-D-*lyxo*-hexopyranos-4-ulose (GDP-4″-keto-mannose) at C5″ and C6″ to form a GDP-6-deoxy-β-L-*erythro*-hex-5-enopyranos-4-ulose (GDP-4″-keto-mannos-5″,6″-ene) intermediate. Reduction of this intermediate by NADPH at C6″ gives the product and regenerates $NADP^+$.[7,8]

The dehydratase reaction has drawn much interest in structural[2,7,9−20] and biochemical studies[7,8,10,19,21−27] spanning several decades to elucidate the enzymatic mechanism. Sugar 4,6-dehydratases are members of the short-chain dehydrogenase/reductase protein superfamily.[28] Their active sites are equipped with the basic SDR (short-chain dehydrogenase and reductase) catalytic apparatus for oxidation−reduction by NAD(P), which has been well characterized from other enzymes.[22,29,30] Accordingly, central problem in our mechanistic understanding of the dehydratase reaction is to elucidate how enzymes integrate a unique β-elimination of water with an apparently "classical" SDR cycle of catalytic hydride transfer to and from NAD(P).[10,13,24,23,31] However, the switch from alcohol oxidation in the first step of the catalytic reaction to C−C double-bond reduction in the last step (Figure 1a) is another unique feature of the sugar 1,4-dehydratases that is not well understood mechanistically.[10]

Chemically, β-elimination of a ketone by enzyme catalysis is likely to proceed stepwise, with Cα-H bond cleavage before the

Received: January 7, 2019
Revised: February 22, 2019
Published: March 1, 2019

DOI: 10.1021/acscatal.9b00064
ACS Catal. 2019, 9, 2962−2968

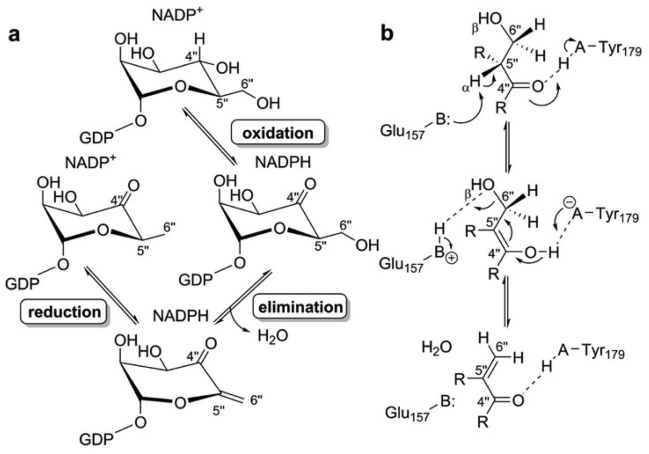

Figure 1. Mechanistic basis for 4,6-dehydration of GDP-mannose by human GDP-mannose 4,6-dehydratase (hGMD). (a) The proposed enzymatic mechanism in three catalytic steps. (b) Stepwise mechanism of β-elimination of water from a ketone.[31]

Cβ-O bond cleavage. Considering thermodynamic requirements for the Cα-H bond cleavage, Gerlt and Gassman[31] refuted enzymatic reaction via base-catalyzed abstraction of the α-proton to form a carbanion (enolate). They proposed a concerted general acid–general base-catalyzed formation of an enol intermediate from which 1,4-elimination of the β-substituent could occur (Figure 1b). They also considered that, given suitable geometry of the enzyme–substrate complex as shown in Figure 1b, the conjugate acid of the base catalyzing the enol formation could also catalyze expulsion of the β-substituent. The proposed mechanism implies a *syn* stereochemical course for the β-elimination reaction and suggests two as the minimal number of functional groups required for efficient catalysis. Herein, we sought to clarify through study of the human GMD (UniProt accession ID: O60547), whether—and if so to what extent—Gerlt and Gassman's minimum catalytic principle for β-elimination[31] was in fact incorporated by an actual sugar 1,4-dehydratase that has emerged from evolution through natural selection. We show, based on high-resolution pre- and postcatalytic complex structures of the enzyme, that human GDP-mannose 4,6-dehydratase (hGMD) represents a perfect realization of that principle in its most parsimonious form. We suggest that other sugar 1,4-dehydratases like dTDP-glucose 4,6-dehydratase[13,24] employ the same principle, but in an expanded version.

Our mechanistic analysis builds on four high-resolution crystal structures of hGMD determined in this study (Table S1, Figure 2): the wildtype enzyme in complex with the inactive substrate analogue GDP-4″-deoxy-4″-fluoro-mannose (PDB: 6GPJ, 1.94 Å); the inactive E157Q variant in complex

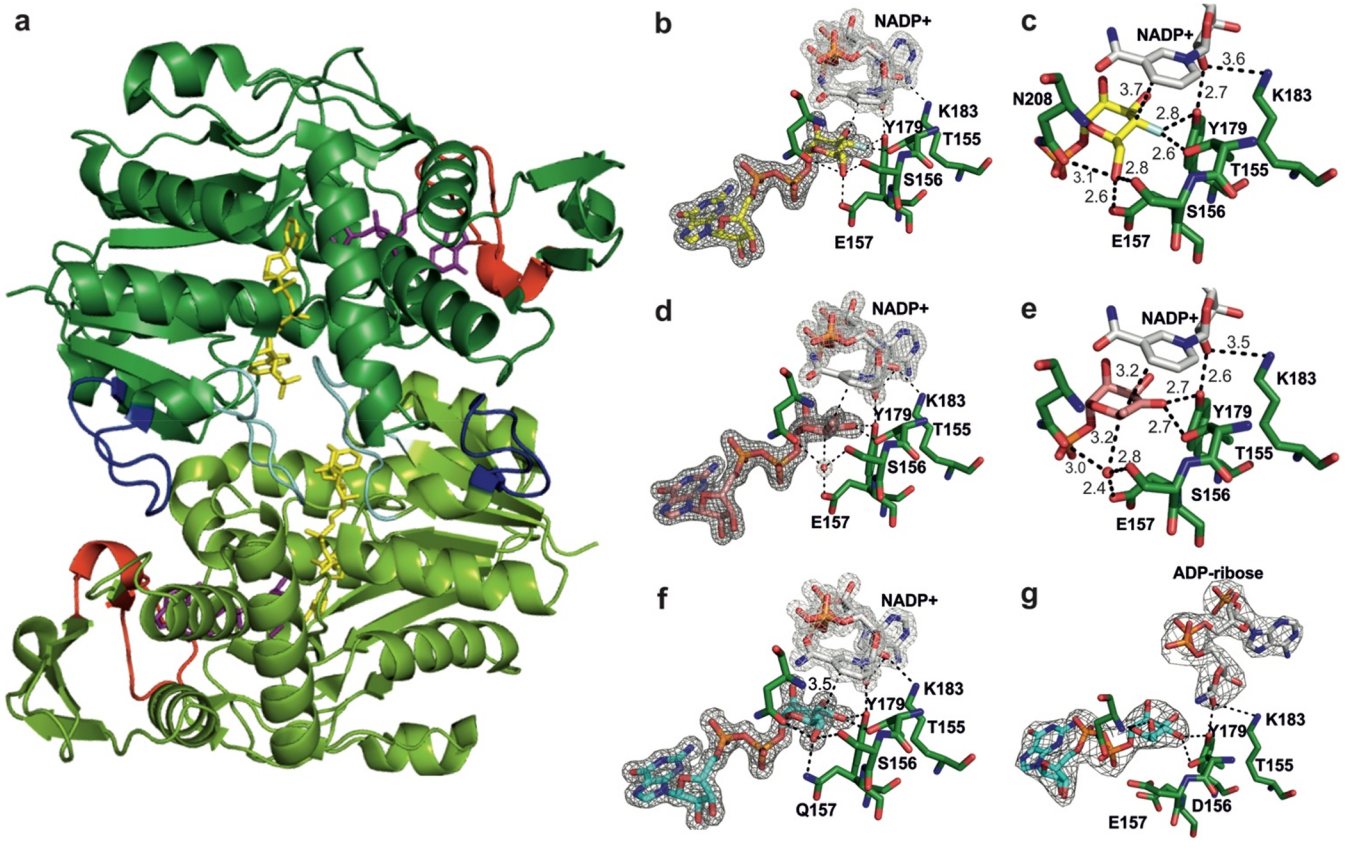

Figure 2. High-resolution crystal structures of hGMD. (a) Overall fold of the hGMD dimer (E157Q variant); each monomer has bound GDP-mannose (purple) and NADP$^+$ (yellow). The NADP$^+$ binding loop (cyan), the substrate binding loop (red) and allosteric inhibitor (GDP-L-fucose) binding loop (dark blue) are highlighted. (b–g) Close-up structures of (b,c) wildtype hGMD bound with GDP-4″-deoxy-4″-fluoro-mannose (yellow), (d,e) wildtype hGMD bound with the product GDP-4″-keto-6″-deoxy-mannose (salmon), (f) E157Q variant bound with GDP-mannose (cyan) and (g) S156D variant bound with GDP-mannose (cyan) and ADP-ribose, a cleavage product of NADP$^+$ (white). Hydrogen bonds are shown as dashed black lines, with distances indicated in Å. The $2F_O-F_C$ electron density maps of the final structure (gray) are contoured at 2σ and are clipped around the ligands.

DOI: 10.1021/acscatal.9b00064
ACS Catal. 2019, 9, 2962–2968

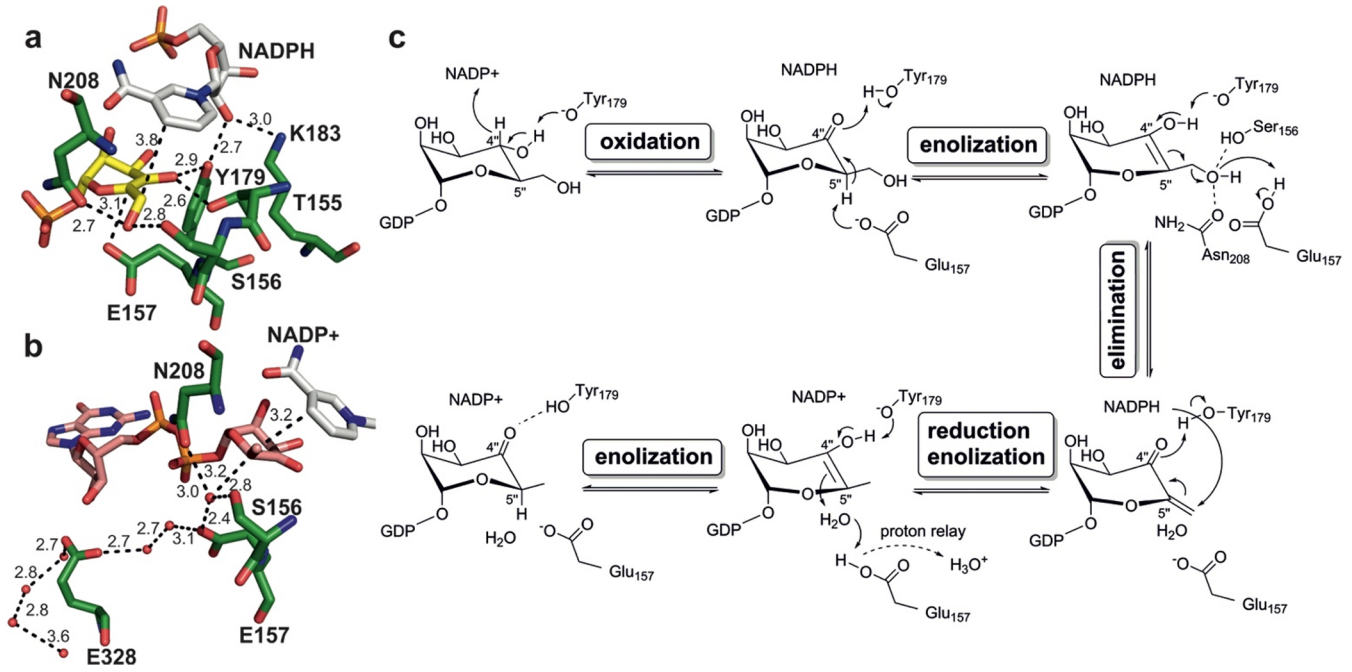

Figure 3. Proposed catalytic mechanism of hGMD. (a) Proton abstraction from the C5″ by Glu157 is suggested by results of molecular dynamics simulations. A structure snapshot (3.1 ns) of the complex of wildtype hGMD bound with NADPH and GDP-mannos-4″,5″-ene shows Glu157 in a position suitable for proton transfer. (b) Proton relay or proton uptake from bulk water in the final ketone-forming step of the reaction is shown. (c) Detailed proposal of the catalytic mechanism.

with GDP-mannose (PDB: 6GPK, 1.47 Å); the wildtype enzyme in complex with the product GDP-4″-keto-6″-deoxy-mannose (PDB: 6GPL, 1.76 Å); and the S156D variant in complex with GDP-mannose and ADP-ribose (PDB: 6Q94, 2.8 Å). In capturing at atomic resolution the start and end point of the enzymatic reaction, these structures together with biochemical data and evidence from molecular dynamics simulation make detailed suggestion for the catalytic path from substrate to product. It is exactly this important fundamental insight which has been difficult to obtain from previous structural studies on sugar 1,4-dehydratases that could reveal the enzyme−substrate complex[13,15,16] or enzyme complexes with substrate/product analogue.[13,14,17]

Crystals of hGMD (Figure 2a) contain two to four homodimers in the asymmetric unit, with subunits arranged side to side in an opposite up-and-down orientation. Each subunit adopts the characteristic SDR fold, composed of a prominent Rossman-fold domain for $NADP^+$ binding to which a smaller GDP-Man binding domain is appended (for a detailed structural description, see Figures S3 and S4). The active site is in a cleft at the interface of the two domains. The two actives sites are separate one from another in the dimer structure (Figure 2a), apparently functioning independently in catalysis. However, there is cooperativity between the subunits for tight binding of $NADP^+$. The loop of residues 55−63 extends into the neighboring subunit and locks down on the $NADP^+$ bound (Figure S3), as seen similarly in prokaryotic and plant GMDs.[14,18] Movement away by this loop and dimer disruption would be necessary for $NADP^+$ to dissociate. The E157Q structure captures the loop (residues 70−78) for binding of the allosteric inhibitor GDP-L-fucose in the same conformation as shown in the GDP-L-fucose complex of wildtype hGMD[32] (Figure 2a; for details, see Figure S4), despite the fact that no GDP-L-fucose is present. The inhibitor loop is disordered in the two wildtype structures reported here.

Although not the main focus of this study, the result bears immediate significance for hGMD inhibition. Conformational sampling, rather than induced fit, by GDP-L-fucose is suggested as the structural principle of inhibitor binding in hGMD. The inhibition entails cooperativity between the protein subunits, as shown in Figure S4. Its mechanistic basis is that GDP-L-fucose binding blocks the entrance to the GDP-mannose binding pocket of the opposing chain.

For structural characterization of the hGMD Michaelis complex (Figure 2b,c), we first targeted the native enzyme. In search for an unreactive substrate analog, we considered substituting the 4-hydroxy group of α-mannosyl with fluorine. While rendering the substrate incompetent for catalytic turnover, the substitution arguably causes only weak perturbation of the enzyme−substrate interactions originally present.[33−35] We therefore developed a synthesis for GDP-4″-deoxy-4″-fluoro-mannose (Figure S5) and show with isothermal titration calorimetry (ITC; Figure S6) that the fluorinated ligand binds to hGMD with a dissociation constant (K_d) of 1.6 (±0.1) μM, comparable to the 8 (±1) μM K_m (~K_d, vide infra) for GDP-mannose. In a second approach, we targeted the native substrate, necessitating the construction of an inactive hGMD variant (E157Q). The atomic maps of catalytic center interactions shown in the wildtype complex with GDP-4″-deoxy-4″-fluoro-mannose (Figure 2b,c) and in the E157Q complex with GDP-mannose (Figure 2f) are consistent and are mutually supportive in suggesting a positioning of the substrate for catalysis. This demonstrates important complementarity in the approaches used.

The hGMD active site is composed of a canonical SDR catalytic triad (Tyr_{179}, Thr_{155}, Lys_{183}) for alcohol oxidation by $NADP^+$, extended by three residues (Glu_{157}, Ser_{156}, Asn_{208}) promoting β-elimination. Tyr_{179} and Thr_{155} each form a hydrogen bond with the substituent at α-mannosyl C4″ (fluorine, Figure 2b,c; hydroxy, Figure 2f; overlay in Figure

DOI: 10.1021/acscatal.9b00064
ACS Catal. 2019, 9, 2962−2968

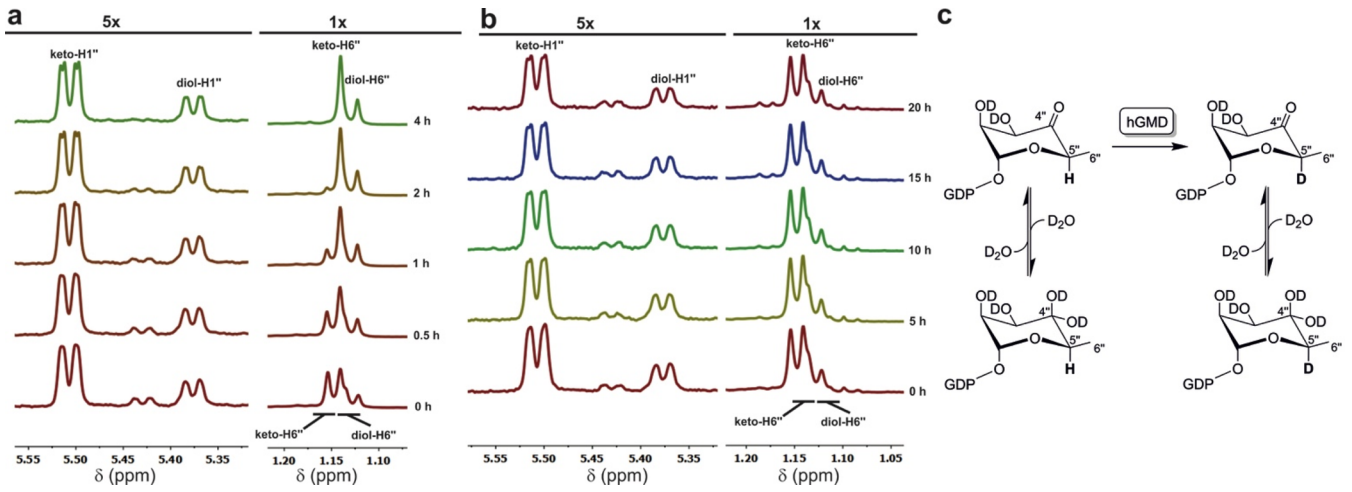

Figure 4. In situ ^{1}H NMR monitoring of deuterium incorporation from solvent into C5″ of GDP-4″-keto-6″-deoxy-mannose (3 mM) on incubation with (a) 1.4 μM wildtype hGMD or (b) 71 μM E157Q variant. (a) The H6″ doublets of GDP-4″-keto-6″-deoxy-mannose (keto-H-6″) and the corresponding hydrate (C4″-diol) are gradually transformed to singlets, indicating deuterium incorporation at C5″ catalyzed by wildtype hGMD. Note: signal change from doublet to singlet for H6″ was more conveniently analyzed than signal decrease for H5″. The signal for H5″ was partly overlapped in the 1H-NMR spectra of GDP-4″-keto-6″-deoxy-mannose. (b) The H6″ doublets remain unchanged during incubation with the E157Q variant, indicating the absence of deuterium incorporation at C5″. (c) Deuterium incorporation at C5″ catalyzed by hGMD and spontaneous formation of the 4″-diol form of GDP-4″-keto-6″-deoxy-mannose in aqueous solution (here D_2O). At equilibrium, the 4″-keto and 4″-diol forms are present at a ratio of about 3:1.

S7a). The nicotinamide C4 is above the substrate C4″, with distance (3.5−3.7 Å) and angle (77°−83°; relative to the nicotinamide ring C4−N1 axis) well set for hydride transfer.[9,10] Lys_{183} establishes a highly conserved SDR proton relay:[36] a chain of hydrogen bonds connects Tyr_{179} (the catalytic acid/base) via the ribosyl hydroxy group and the ε-amino group of lysine to water (Figure S8). The hGMD is special in that its proton relay does not connect to bulk water, but ends in a reservoir of water molecules buried inside the protein (Figure S8). Glu_{157}, Ser_{156}, and Asn_{208} each forms a hydrogen bond with the C6″ hydroxy group. The orientation of the hydroxy group is in accordance with a β-elimination having *syn* stereochemical course.

The structure of hGMD bound with the GDP-4″-keto-6″-deoxy-mannose (Figure 2d,e) suggests a true postcatalytic complex captured in the crystal. A water molecule, likely the one eliminated from the C6″, is held in place by Glu_{157}, Ser_{156}, and Asn_{208}. The nicotinamide C4 is positioned above the C6″, with distance (3.2 Å) and angle (116°; relative to the C4−N1 axis) both proper for hydride transfer. Tyr_{179} and Thr_{155} form a hydrogen bond (2.7 Å each) with the C4″ keto group of product. Comparing the product (Figure 2d,e) to the substrate complex structure (Figure 2b,c), the product C6″ has made a 1.1 Å upward movement and is now favorably positioned for hydride transfer to the coenzyme (Figure S9). Apart from this subtle change, all atomic positions defining the catalytic center interactions are effectively the same in substrate and product complex (Figure S7; Figure S9). Therefore, hGMD seems to accommodate the different catalytic steps of its overall reaction (Figure 1a) without the need for repositioning of the enzyme and substrate groups, thus conforming to the "principle of least nuclear motion" in enzyme catalysis. The central, nearly parallel orientation of the nicotinamide ring to the sugar ring plane determines the strict 1,4-reductive regioselectivity of hGMD. In contrast, as pointed out in study of the hexosamine nucleotide 5,6-dehydratase TunA, a 1,2-selective hydride addition (to reduce the 4″-keto moiety) would necessitate the ring planes to lie in certain angle (observed: 22°) to each other.[19]

Gerlt and Gassman's mechanism (Figure 1b) built into hGMD implies a 4,5-enolization of GDP-4″-keto-mannose under concerted general acid−general base catalysis from Tyr_{179} and Glu_{157}, respectively.[37] In both enzyme structures reporting on the Michaelis complex (Figure 2b,f), however, the Glu_{157} is hydrogen bonded to the C6″ hydroxy group. Molecular dynamics simulations of enzyme complex with NADPH and the enol (GDP-mannos-4″,5″-ene) intermediate show that in 21% of 150 structure snapshots analyzed over a total runtime of 15 ns, the Glu_{157} approaches the C5″ at a distance (~3.5 Å) plausible for catalytic proton transfer at this position (Figure 3a, for details, see Figures S12 and S13 as well as Table S2).[38] In the remainder time of the simulation, the Glu_{157} is in contact with the C6″ hydroxy group. The side-chain conformational flexibility thus revealed is essential for Glu_{157} to function as catalytic base during the enol formation and, in conjugate acid form, as catalytic acid during the expulsion of water, as proposed in Figure 3a,c.

With β-elimination complete, the conversion of the GDP-4″-keto-mannos-5″,6″-ene intermediate to the GDP-4″-keto-6″-deoxy-mannose product likely proceeds in two steps, representing in opposite order the reversal of the previous catalytic steps of oxidation and enolization (Figure 3c). Accordingly, hydride reduction at C6″ proceeds under catalytic facilitation by Tyr_{179} as the general acid and gives the 4,5-enol (Figure 3c), consistent with computational analysis of a small-molecule model of the dehydratase reduction step.[10] The ketone formation involves concerted catalysis by Tyr_{179} and Glu_{157} and results in proton transfer from water via Glu_{157} to the C5″. Our structural analysis of hGMD reveals the path of proton uptake from bulk water (Figure 3b), and it shows this previously unrecognized path to be largely conserved in other sugar dehydratases (Figure S11).

Mutagenesis combined with measurement of C5″ deuterium exchange, using method adopted from Gross et al.,[23] provides

DOI: 10.1021/acscatal.9b00064
ACS Catal. 2019, 9, 2962−2968

biochemical support to the mechanistic claim that Tyr_{179} and Glu_{157} provide concerted catalysis to enol formation. We show with in situ proton NMR that upon incubation in D_2O in the presence of the GDP-4″-keto-6″-deoxy-mannose product, the wildtype enzyme catalyzes rapid "wash-in" of solvent deuterium at C5″ (Figure 4a,c, Table 1) while E157Q (Figure 4b, Table 1) and Y179F are inactive (Figure S27, Table 1).

Table 1. Kinetic Parameters and NADPH Content of hGMD and Variants Thereof

enzyme	k_{cat} [s^{-1}][a]	K_M [μM][a]	NADPH content (%)	deuterium incorporation [s^{-1}][d]
WT	0.42 ± 0.08	8 ± 1	3[b]/n.d.[c]	0.28 (fast)
Y179F	n.d.	n.d.	70/n.d.	n.d
E157Q	n.d.	n.d.	49/n.d.	n.d
S156D	n.d.	n.d.	15/n.d.	0.13 (medium)
S156A	0.05 ± 0.01	127 ± 5	8/n.d.	0.01 (slow)

[a]From initial rate measurements at 37 °C. [b,c]Mol NADPH/mol enzyme subunit, expressed in percent, in the enzyme as isolated. [b]and in the enzyme at steady state during reaction with GDP-Man. [c]. For the methods used, see the Supporting Information. [d]Deuterium exchange rates measured with in situ ^{1}H NMR spectroscopy in D_2O at 30 °C and determined from the integrated signal of 6H″ in GDP-4″-keto-6″-deoxy-mannose, GDP-4″-diol-6″-deoxy-mannose, GDP-4″-keto-5″-deutero-6″-deoxy-mannose and GDP-4″-diol-5″-deutero-6″-deoxy-mannose. n.d., not detectable.

Having shown that hGMD represents, in a most elementary form, Gerlt and Gassman's chemical principle of catalytic β-elimination of a ketone (cf. Figure 1b and Figure 3c), we investigated a conspicuous structural variation in sugar 1,4-dehydratase active sites: dTDP-glucose dehydratase has an aspartic acid residue[13,23,24] in place of Ser_{156} in hGMD (Figure S10). We find that the S156D variant of hGMD is inactive toward GDP-mannose but promotes C5″ deuterium exchange in GDP-4″-keto-6″-deoxy-mannose at half the rate of the wildtype enzyme (Figure S28, Table 1). The structure of S156D in complex with GDP-mannose (2.8 Å; Figure 2e, Table S1) shows electron density for the substrate and for 2′-phospho-ADP-ribose (a cleavage product of $NADP^+$). Lacking coordination with Asp_{156}, the C6″ hydroxy group of GDP-mannose adopts a pseudoaxial position which conflicts with the presence of the nicotinamide ring. Although redox chemistry is thus rendered impossible for the S156D variant, its Tyr_{179} and Glu_{157} are in plausible positions to catalyze enol formation in the product. We additionally show that a S156A variant retains activity with GDP-mannose (12% of wildtype, Figure S26) but is much slower (13-fold) in C5″ deuterium exchange (Figure S29, Table 1) than the S156D variant. It is also significant that hGMD turns over at a ∼10-fold slower rate (k_{cat} = 0.42 s^{-1}; Table 1, Figure S25) than dTDP-glucose dehydratase does.

In hGMD, the reduced NADPH form of the enzyme is not detectably present in the reaction at steady state (Figure S18). The k_{cat} is therefore limited by a substrate oxidation that either is slow intrinsically or occurs kinetically coupled to a subsequent step, likely the enolization, that leads to an internal equilibrium far on the side of enzyme-bound GDP-mannose. Although beyond the scope of the current investigation, kinetic isotope effects could be useful to distinguish between these kinetic scenarios for hGMD. In contrast to hGMD, the 4.9 s^{-1} k_{cat} of dTDP-glucose dehydratase is limited partly by dTDP-4″,5″-glucosene reduction[25] and the reaction involves enzyme-NADH (45% of total)[27] at steady state. On the basis of these considerations, we think that nature's mechanistic rationale for having Asp instead of Ser in the 4,6-dehydratase catalytic apparatus might have been to drive the oxidation-enolization by making proton abstraction from C5″ to the enzyme thermodynamically more favorable, as shown in Figure S30. With the pK_a of the catalytic Glu increased in the presence of the neighboring Asp, as analogously observed in other enzymes,[39−41] the energetic barrier to the enol formation might be reduced effectively. A speeding up of the catalytic reaction thus achievable might benefit the enzyme function in particular physiological contexts.

In summary, therefore, this mechanistic account of hGMD advances the detailed understanding of hexose dehydration by a class of sugar 1,4-dehydratases. This is broadly relevant regarding the enzymology of 6-deoxy-sugar biosynthesis. It also provides important insight into the evolution of enzyme structure, function, and mechanism in a superfamily wide context of short-chain dehydrogenases/reductases.

■ ASSOCIATED CONTENT

Supporting Information

The Supporting Information is available free of charge on the ACS Publications website at DOI: 10.1021/acscatal.9b00064.

Experimental methods used; enzyme purification and crystallization (Figures S1 and S2); enzyme crystal structures and biochemical characterization (Figures S3−S11, Table S1); MD simulation results (Figures S12 and S13, Table S2); reaction kinetic analysis (Figure S14−S18); NMR data (Figures S19−S24); in situ NMR analysis of deuterium exchange (Figures S25−S29); proposed elimination mechanism in hGMD and dTDP-glucose 4,6-dehydratase (Figure S30); and associated references (PDF)

■ AUTHOR INFORMATION

Corresponding Author

*E-mail: bernd.nidetzky@tugraz.at.

ORCID

Udo Oppermann: 0000-0001-9984-5342

Bernd Nidetzky: 0000-0002-5030-2643

Notes

The authors declare no competing financial interest.

■ ACKNOWLEDGMENTS

The authors thank A. Oberecker (Graz University of Technology) for experiments; Prof. H. Weber (Graz University of Technology) for NMR measurements; Dr. M. Kitaoka (National Food Research Institute, Japan) for the NahK expression plasmid; the Diamond Light Source for beamtime (proposal mx-15433) and the staff of beamlines I03, I04-1 and I24 for assistance with crystyal testing and data collection; and Prof Lothar Brecker (University of Vienna) for discussion of the carbohydrate nomenclature. Financial support from the Austrian Science Funds (FWF, DK Molecular Enzymology W901; to B.N. and M.P.) is gratefully acknowledged. The work in Oxford was supported by Oxford NIHR Biomedical Research Centre and Arthritis Research UK (20522). The SGC (charity no. 1097737) receives funds from AbbVie, Bayer Pharma AG, Boehringer Ingelheim, Canada Foundation for

DOI: 10.1021/acscatal.9b00064
ACS Catal. 2019, 9, 2962−2968

Innovation, Eshelman Institute for Innovation, Genome Canada, Innovative Medicines Initiative (EU/EFPIA) [ULTRA-DD grant no. 115766], Janssen, Merck KGaA Darmstadt Germany, MSD, Novartis Pharma AG, Ontario Ministry of Economic Development and Innovation, Pfizer, São Paulo Research Foundation-FAPESP, Takeda, Wellcome [106169/ZZ14/Z]. Funding was received from People Programme (Marie Curie Actions) of the European Union's Seventh Framework Programme (FP7/2007-2013) under REA grant agreement no. [609305].

REFERENCES

(1) Li, J.; Hsu, H. C.; Mountz, J. D.; Allen, J. G. Unmasking Fucosylation: From Cell Adhesion to Immune System Regulation and Diseases. *Cell Chem. Biol.* **2018**, *25*, 499−512.

(2) Singh, S.; Phillips, G. N., Jr.; Thorson, J. S. The Structural Biology of Enzymes Involved in Natural Product Glycosylation. *Nat. Prod. Rep.* **2012**, *29*, 1201−1237.

(3) Thibodeaux, C. J.; Melançon, C. E.; Liu, H. Unusual Sugar Biosynthesis and Natural Product Glycodiversification. *Nature* **2007**, *446*, 1008−1016.

(4) Bisso, A.; Sturla, L.; Zanardi, D.; De Flora, A.; Tonetti, M. Structural and Enzymatic Characterization of Human Recombinant GDP-D-Mannose-4,6-Dehydratase. *FEBS Lett.* **1999**, *456*, 370−374.

(5) Sturla, L.; Bisso, A.; Zanardi, D.; Benatti, U.; De Flora, A.; Tonetti, M. Expression, Purification and Characterization of GDP-D-Mannose 4, 6-Dehydratase from *Escherichia coli*. *FEBS Lett.* **1997**, *412*, 126−130.

(6) Tonetti, M.; Sturla, L.; Bisso, A.; Benatti, U.; De Flora, A. Synthesis of GDP-L-Fucose by the Human FX Protein. *J. Biol. Chem.* **1996**, *271*, 27274−27279.

(7) Somoza, J. R.; Menon, S.; Schmidt, H.; Joseph-McCarthy, D.; Dessen, A.; Stahl, M. L.; Somers, W. S.; Sullivan, F. X. Structural and Kinetic Analysis of *Escherichia coli* GDP-Mannose 4, 6 Dehydratase Provides Insights into the Enzyme's Catalytic Mechanism and Regulation by GDP-Fucose. *Structure* **2000**, *8*, 123−135.

(8) Oths, P. J.; Mayer, R. M.; Floss, H. G. Stereochemistry and Mechanism of the GDP-Mannose Dehydratase Reaction. *Carbohydr. Res.* **1990**, *198*, 91−100.

(9) Allard, S. T.; Giraud, M. F.; Whitfield, C.; Graninger, M.; Messner, P.; Naismith, J. H. The Crystal Structure of dTDP-D-Glucose 4,6-Dehydratase (RmlB) from *Salmonella Enterica* Serovar *Typhimurium*, the Second Enzyme in the dTDP-L-Rhamnose Pathway. *J. Mol. Biol.* **2001**, *307*, 283−295.

(10) Beis, K.; Allard, S. T. M.; Hegeman, A. D.; Murshudov, G.; Philp, D.; Naismith, J. H. The Structure of NADH in the Enzyme dTDP-D-Glucose Dehydratase (RmlB). *J. Am. Chem. Soc.* **2003**, *125*, 11872−11878.

(11) Vogan, E. M.; Bellamacina, C.; He, X.; Liu, H.; Ringe, D.; Petsko, G. A. Crystal Structure at 1.8 Å Resolution of CDP-D-Glucose 4,6-Dehydratase from *Yersinia pseudotuberculosis*. *Biochemistry* **2004**, *43*, 3057−3067.

(12) King, J. D.; Poon, K. K. H.; Webb, N. A.; Anderson, E. M.; McNally, D. J.; Brisson, J.-R.; Messner, P.; Garavito, R. M.; Lam, J. S. The Structural Basis for Catalytic Function of GMD and RMD, Two Closely Related Enzymes from the GDP-D-Rhamnose Biosynthesis Pathway. *FEBS J.* **2009**, *276*, 2686−2700.

(13) Allard, S. T.; Beis, K.; Giraud, M.-F.; Hegeman, A. D.; Gross, J. W.; Wilmouth, R. C.; Whitfield, C.; Graninger, M.; Messner, P.; Allen, A. G.; Maskell, D. J.; Naismith, J. H. Toward a Structural Understanding of the Dehydratase Mechanism. *Structure* **2002**, *10*, 81−92.

(14) Mulichak, A. M.; Bonin, C. P.; Reiter, W.-D.; Garavito, R. M. Structure of the MUR1 GDP-Mannose 4,6-Dehydratase from *Arabidopsis Thaliana*: Implications for Ligand Binding and Specificity. *Biochemistry* **2002**, *41*, 15578−15589.

(15) Allard, S. T. M.; Cleland, W. W.; Holden, H. M. High Resolution X-Ray Structure of dTDP-Glucose 4,6-Dehydratase from *Streptomyces venezuelae*. *J. Biol. Chem.* **2004**, *279*, 2211−2220.

(16) Riegert, A. S.; Thoden, J. B.; Schoenhofen, I. C.; Watson, D. C.; Young, N. M.; Tipton, P. A.; Holden, H. M. Structural and Biochemical Investigation of PglF from *Campylobacter jejuni* Reveals a New Mechanism for a Member of the Short Chain Dehydrogenase/Reductase Superfamily. *Biochemistry* **2017**, *56*, 6030−6040.

(17) Koropatkin, N. M.; Holden, H. M. Structure of CDP-D-Glucose 4,6-Dehydratase from *Salmonella typhi* Complexed with CDP-D-Xylose. *Acta Crystallogr., Sect. D: Biol. Crystallogr.* **2005**, *61*, 365−373.

(18) Webb, N. A.; Mulichak, A. M.; Lam, J. S.; Roccetta, H. L.; Garavito, M. R. Crystal Structure of a Tetrameric GDP-D-Mannose 4,6-Dehydratase from a Bacterial GDP-D-Rhamnose Biosynthetic Pathway. *Protein Sci.* **2004**, *13*, 529−539.

(19) Wyszynski, F. J.; Lee, S. S.; Yabe, T.; Wang, H.; Gomez-Escribano, J. P.; Bibb, M. J.; Lee, S. J.; Davies, G. J.; Davis, B. G. Biosynthesis of the Tunicamycin Antibiotics Proceeds via Unique Exo-Glycal Intermediates. *Nat. Chem.* **2012**, *4*, 539−546.

(20) Ishiyama, N.; Creuzenet, C.; Miller, W. L.; Demendi, M.; Anderson, E. M.; Harauz, G.; Lam, J. S.; Berghuis, A. M. Structural Studies of FlaA1 from *Helicobacter pylori* Reveal the Mechanism for Inverting 4,6-Dehydratase Activity. *J. Biol. Chem.* **2006**, *281*, 24489−24495.

(21) Okazaki, R.; Okazakit, N.; Strominger, J. L.; Michelson, A. M. Thymidine Diphosphate 4-Keto-6-Deoxy-D-Glucose, an Intermediate in Thymidine Diphosphate L-Rhamnose Synthesis in *Escherichia coli* Strains. *J. Biol. Chem.* **1962**, *237*, 3014−3026.

(22) Gerratana, B.; Cleland, W. W.; Frey, P. A. Mechanistic Roles of Thr134, Tyr160, and Lys 164 in the Reaction Catalyzed by dTDP-Glucose 4,6-Dehydratase. *Biochemistry* **2001**, *40*, 9187−9195.

(23) Gross, J. W.; Hegeman, A. D.; Gerratana, B.; Frey, P. A. Dehydration Is Catalyzed by Glutamate-136 and Aspartic Acid-135 Active Site Residues in *Escherichia coli* dTDP-Glucose 4,6-Dehydratase. *Biochemistry* **2001**, *40*, 12497−12504.

(24) Hegeman, A. D.; Gross, J. W.; Frey, P. A. Concerted and Stepwise Dehydration Mechanisms Observed in Wild-Type and Mutated *Escherichia coli* dTDP-Glucose 4,6-Dehydratase. *Biochemistry* **2002**, *41*, 2797−2804.

(25) Gross, J. W.; Hegeman, A. D.; Vestling, M. M.; Frey, P. A. Characterization of Enzymatic Processes by Rapid Mix−Quench Mass Spectrometry: The Case of dTDP-Glucose 4,6-Dehydratase. *Biochemistry* **2000**, *39*, 13633−13640.

(26) Hallis, T. M.; Liu, H. Learning Nature's Strategies for Making Deoxy Sugars: Pathways, Mechanisms, and Combinatorial Applications. *Acc. Chem. Res.* **1999**, *32*, 579−588.

(27) Hegeman, A. D.; Gross, J. W.; Frey, P. A. Probing Catalysis by *Escherichia Coli* dTDP-Glucose-4,6-Dehydratase: Identification and Preliminary Characterization of Functional Amino Acid Residues at the Active Site. *Biochemistry* **2001**, *40*, 6598−6610.

(28) Kavanagh, K. L.; Jörnvall, H.; Persson, B.; Oppermann, U. Medium- and Short-Chain Dehydrogenase/reductase Gene and Protein Families: The SDR Superfamily: Functional and Structural Diversity within a Family of Metabolic and Regulatory Enzymes. *Cell. Mol. Life Sci.* **2008**, *65*, 3895−3906.

(29) Thoden, J. B.; Wohlers, T. M.; Fridovich-Keil, J. L.; Holden, H. M. Crystallographic Evidence for Tyr 157 Functioning as the Active Site Base in Human UDP-Galactose 4-Epimerase. *Biochemistry* **2000**, *39*, 5691−5701.

(30) Liu, Y.; Thoden, J. B.; Kim, J.; Berger, E.; Gulick, A. M.; Ruzicka, F. J.; Holden, H. M.; Frey, P. A. Mechanistic Roles of Tyrosine 149 and Serine 124 in UDP-Galactose 4-Epimerase from *Escherichia coli*. *Biochemistry* **1997**, *36*, 10675−10684.

(31) Gerlt, J. A.; Gassman, P. G. Understanding Enzyme-Catalyzed Proton Abstraction from Carbon Acids: Details of Stepwise Mechanisms for β-Elimination Reactions. *J. Am. Chem. Soc.* **1992**, *114*, 5928−5934.

(32) Allen, J. G.; Mujacic, M.; Frohn, M. J.; Pickrell, A. J.; Kodama, P.; Bagal, D.; San Miguel, T.; Sickmier, E. A.; Osgood, S.; Swietlow,

DOI: 10.1021/acscatal.9b00064
ACS Catal. 2019, 9, 2962−2968

A.; Li, V.; Jordan, J. B.; Kim, K. W.; Rousseau, A. C.; Kim, Y. J.; Caille, S.; Achmatowicz, M.; Thiel, O.; Fotsch, C. H.; Reddy, P.; McCarter, J. D. Facile Modulation of Antibody Fucosylation with Small Molecule Fucostatin Inhibitors and Cocrystal Structure with GDP-Mannose 4,6-Dehydratase. *ACS Chem. Biol.* **2016**, *11*, 2734−2743.

(33) Chapeau, M.-C.; Frey, P. A. Synthesis of UDP-4-Deoxy-4-Fluoroglucose and UDP-4-Deoxy-4-Fluorogalactose and Their Interactions with Enzymes of Nucleotide Sugar Metabolism. *J. Org. Chem.* **1994**, *59*, 6994−6998.

(34) Thoden, J. B.; Hegeman, A. D.; Wesenberg, G.; Chapeau, M. C.; Frey, P. A.; Holden, H. M. Structural Analysis of UDP-Sugar Binding to UDP-Galactose 4-Epimerase from *Escherichia coli*. *Biochemistry* **1997**, *36*, 6294−6304.

(35) Hoffmann, M.; Rychlewski, J. Effects of Substituting a OH Group by a F Atom in D-Glucose. Ab Initio and DFT Analysis. *J. Am. Chem. Soc.* **2001**, *123*, 2308−2316.

(36) Filling, C.; Berndt, K. D.; Benach, J.; Knapp, S.; Prozorovski, T.; Nordling, E.; Ladenstein, R.; Jörnvall, H.; Oppermann, U. Critical Residues for Structure and Catalysis in Short-Chain Dehydrogenases/Reductases. *J. Biol. Chem.* **2002**, *277*, 25677−25684.

(37) The Tyr179 is ideally positioned to function as the catalytic general acid. Studies of the related dTDP-glucose dehydratase[18] suggest a pK_a for the enzyme tyrosine (pK_a ∼ 6.6) well suited for protonation of the incipient enol (pK_a ∼ 11).

(38) With an equilibrium lying far on the side of ketone, the enolization is expected from the Hammond postulate to involve a product (enol)-like transition state (see ref 31). We therefore used GDP-mannos-4,5-ene for our molecular dynamics simulations.

(39) Meekrathok, P.; Kukic, P.; Nielsen, J. E.; Suginta, W. Investigation of Ionization Pattern of the Adjacent Acidic Residues in the DXDXE Motif of GH-18 Chitinases Using Theoretical pK_a Calculations. *J. Chem. Inf. Model.* **2017**, *57*, 572−583.

(40) Van Aalten, D. M.; Komander, D.; Synstad, B.; Gåseidnes, S.; Peter, M. G.; Eijsink, V. G. Structural Insights into the Catalytic Mechanism of a Family 18 Exo-Chitinase. *Proc. Natl. Acad. Sci. U. S. A.* **2001**, *98*, 8979−8984.

(41) Greig, I. R.; Zahariev, F.; Withers, S. G. Elucidating the Nature of the *Streptomyces plicatus* Beta-Hexosaminidase-Bound Intermediate Using Ab Initio Molecular Dynamics Simulations. *J. Am. Chem. Soc.* **2008**, *130*, 17620−17628.

DOI: 10.1021/acscatal.9b00064
ACS Catal. 2019, 9, 2962−2968